Atmos. Chem. Phys., 9, 3867–3879, 2009
www.atmos-chem-phys.net/9/3867/2009/
© Author(s) 2009. This work is distributed under
the Creative Commons Attribution 3.0 License.

Atmospheric Chemistry and Physics

Validation of urban NO_2 concentrations and their diurnal and seasonal variations observed from the SCIAMACHY and OMI sensors using in situ surface measurements in Israeli cities

K. F. Boersma[1,2], D. J. Jacob[1], M. Trainic[3], Y. Rudich[3], I. DeSmedt[4], R. Dirksen[2], and H. J. Eskes[2]

[1]Harvard University, School of Engineering and Applied Sciences, 29 Oxford Street, Cambridge, MA 02138, USA
[2]Royal Netherlands Meteorological Inst., Climate Observations Dept., Wilhelminalaan 10, 3732 GK De Bilt, The Netherlands
[3]Weizmann Institute, Department of Environmental Sciences, Rehovot 76100, Israel
[4]Belgian Institute for Space Aeronomy, Avenue Circulaire 3, 1180, Brussels, Belgium

Received: 11 December 2008 – Published in Atmos. Chem. Phys. Discuss.: 10 February 2009
Revised: 28 May 2009 – Accepted: 30 May 2009 – Published: 15 June 2009

Abstract. We compare a full-year (2006) record of surface air NO_2 concentrations measured in Israeli cities to coinciding retrievals of tropospheric NO_2 columns from satellite sensors (SCIAMACHY aboard ENVISAT and OMI aboard Aura). This provides a large statistical data set for validation of NO_2 satellite measurements in urban air, where validation is difficult yet crucial for using these measurements to infer NO_x emissions by inverse modeling. Assuming that NO_2 is well-mixed throughout the boundary layer (BL), and using observed average seasonal boundary layer heights, near-surface NO_2 concentrations are converted into BL NO_2 columns. The agreement between OMI and (13:45) BL NO_2 columns (slope=0.93, n=542), and the comparable results at 10:00 h for SCIAMACHY, allow a validation of the seasonal, weekly, and diurnal cycles in satellite-derived NO_2. OMI and BL NO_2 columns show consistent seasonal cycles (winter NO_2 1.6–2.7× higher than summer). BL and coinciding OMI columns both show a strong weekly cycle with 45–50% smaller NO_2 columns on Saturday relative to the weekday mean, reflecting the reduced weekend activity, and validating the weekly cycle observed from space. The diurnal difference between SCIAMACHY (10:00) and OMI (13:45) NO_2 is maximum in summer when SCIAMACHY is up to 40% higher than OMI, and minimum in winter when OMI slightly exceeds SCIAMACHY. A similar seasonal variation in the diurnal difference is found in the source region of Cairo. The surface measurements in Israel cities confirm this seasonal variation in the diurnal cycle. Using simulations from a global 3-D chemical transport model (GEOS-Chem), we show that this seasonal cycle can be explained by a much stronger photochemical loss of NO_2 in summer than in winter.

Correspondence to: F. Boersma
(boersma@knmi.nl)

1 Introduction

Nitrogen oxides ($NO_x \equiv NO+NO_2$) are of central importance for atmospheric chemistry. They are precursors of tropospheric ozone, aerosol nitrate, and the hydroxyl radical (OH) which is the main atmospheric oxidant. About 2/3 of the global source of NO_x is from fossil fuel combustion (IPCC, 2007) and is concentrated in urban areas. Satellite observations of tropospheric NO_2 columns by solar backscatter from the GOME, SCIAMACHY, and OMI sensors have provided increasing information over the past decade to quantify NO_x emissions and their trends at various scales (e.g. Martin et al. (2003); Richter et al. (2004); Konovalov et al. (2006); Martin et al. (2006); Wang et al. (2007); van der A et al. (2008)). Validating these satellite observations is difficult, however. We show here that long-term surface NO_2 measurements from urban air quality monitoring networks provide valuable validation data and can test the seasonal, weekly, and diurnal variations seen from space by the SCIAMACHY and OMI sensors.

The atmospheric lifetime of NO_x against oxidation is of the order of hours (Liang et al., 1998), resulting in large spatial and temporal variability around source areas. High concentrations are mainly restricted to the boundary layer up to 1–2 km, with rapid drop-off at higher altitudes. Drop-off is particularly sharp for NO_2 because of the decrease of

Published by Copernicus Publications on behalf of the European Geosciences Union.

the NO_2/NO ratio with decreasing temperature (Martin et al., 2004). Validation of NO_2 column measurements from space has relied on aircraft vertical profiles coincident with satellite overpasses to capture the full extent of the column (Heland et al., 2002; Martin et al., 2004, 2006; Bucsela et al., 2008). This is expensive and as a result validation data are few. Horizontal variability over the satellite footprint, aircraft traffic restrictions, and the need to extrapolate from the aircraft floor to the surface can further lead to significant errors in comparing aircraft-derived columns to the satellite column measurements. This is particularly problematic in urban areas which are of prime interest for validation (Boersma et al., 2008b).

Surface observations of NO_2 concentrations in urban areas offer an alternate vehicle for satellite validation. Most developed countries have dense urban monitoring networks for NO_2 because it is a regulated pollutant (Ellis, 1975; Hjellbrekke and Fjæraa, 2008). The standard monitoring instrumentation is subject to interferences from NO_x oxidation products (Winer et al., 1974; Grosjean and Harrison, 1985; Gerboles et al., 2003; Steinbacher et al., 2007; Dunlea et al., 2007; Lamsal et al., 2008), and the lack of vertical information above the surface induces error. On the other hand, the high spatial and temporal density of the data greatly improve the validation statistics (Schaub et al., 2006; Ordóñez et al., 2006; Blond et al., 2007) over what is possible from aircraft profiles. The lack of vertical information in the surface data may in fact be less of a problem than the need to extrapolate aircraft observations down to the surface.

Air pollution in Israel is strongly influenced by the country's unique geographical features (the south/east is influenced by large deserts, the north/west by a Mediterranean climate). Most economic activity and half the population are concentrated in the coastal plain, a less than 15 km wide strip of 170 km length (North-South). The small geographical scale, in combination with the high population density and the high emissions, lead to substantial air pollution, whose pattern and trends are not easily captured by a few ground monitoring stations. Indeed, since the 1990s, mixed emission trends have been observed for different NO_x sources. This unique situation calls for development of remote sensing abilities that compensate for the lack of spatial and temporal scales covered by ground monitoring stations. In this study, we are making first steps towards developing such tools for this region.

2 NO_2 observations

2.1 SCIAMACHY Tropospheric NO_2 columns

We use tropospheric NO_2 columns retrieved from SCIAMACHY on board ESA's ENVISAT. This satellite (launched March 2002) orbits the Earth in a polar, sun-synchronous way in a descending node crossing the equator at approximately 10:00 local time. SCIAMACHY observes the atmosphere alternatingly in nadir and limb viewing modes. Tropospheric information is available from the nadir spectra only. In combination with the SCIAMACHY nadir field-of-view, corresponding to a swath width of 960 km on the Earths surface, this leads to global coverage approximately once every six days. The nadir surface spatial resolution is $30\times60\,km^2$.

We use the SCIAMACHY NO_2 retrievals (v1.1) available from the Tropospheric Emission Monitoring Internet Service (http://www.temis.nl) for the year 2006. The retrieval algorithm has been described in detail in Boersma et al. (2004), and Blond et al. (2007). In brief, slant column densities are determined with Differential Optical Absorption Spectroscopy (DOAS) in the 426.3–451.3 nm spectral window. The stratospheric (background) slant column is estimated from data assimilation of slant columns in the global chemistry-transport model TM4 (Dentener et al., 2003). After subtraction of the stratospheric slant column, the residual tropospheric slant column is translated into a tropospheric vertical column by a tropospheric air mass factor that accounts for viewing geometry, the NO_2 and temperature profile shape, as well as the pressure and reflectivity of clouds and surface. The SCIAMACHY NO_2 retrieval (v1.1) is improved relative to earlier versions (v1.04) because it includes cloud parameters retrieved from FRESCO+. The FRESCO+ algorithm uses a more realistic physical model of the atmosphere by accounting for single Rayleigh scattering, and this leads to higher cloud fractions and cloud pressures. These in turn result in NO_2 columns that are lower for polluted situations with low clouds, leading to better agreement with independent NO_2 validation data (Wang et al., 2008).

Errors in the slant column fitting, the stratospheric correction, and in the air mass factor lead to an overall error in the SCIAMACHY tropospheric NO_2 columns with an absolute component of approximately 0.65×10^{15} molecules cm^{-2} (from the tropospheric slant column) and a relative component of approximately 30% (from the tropospheric air mass factor).

2.2 OMI Tropospheric NO_2 columns

OMI onboard NASA's EOS-Aura satellite (launched July 2004) provides tropospheric NO_2 columns at approximately 13:45 local time. Together with the 10:00 measurements by SCIAMACHY, this provides valuable information on the diurnal cycle in NO_2. OMI also improves on SCIAMACHY because it observes the Earth's atmosphere continuously in nadir mode with a 114° field-of-view (2600 km on the Earth's surface), thereby achieving daily global coverage. Furthermore, the nadir spatial resolution of $13\times24\,km^2$ allows for the observation of finer details, and increases the likelihood of encountering cloud-free scenes (Krijger et al., 2007). We use the DOMINO (Dutch OMI NO_2) product (v1.02) available from http://www.temis.nl for the year 2006. The

Table 1. Summary of the comparison between surface NO_2 concentrations and OMI tropospheric NO_2 columns at 8 Israeli cities in 2006.

Station	Lat. (° N)	Lon. (° E)	r	n	slope (molecules cm^{-2}/ppb)	intercept (molecules cm^{-2})
Carmiel	32.93	35.30	0.52	97	1.33±0.29	−2.62±0.59
Haifa	32.82	34.99	0.65	137	0.30±0.03	−2.23±0.42
Afula	32.65	35.20	0.13	59	0.60±2.75	−0.09±0.82
Modiin	31.92	34.99	0.65	106	1.06±0.11	−1.11±0.91
Rehovot	31.90	34.80	0.77	100	1.13±0.13	0.26±0.60
Ashdod	31.80	34.65	0.54	105	0.59±0.11	−3.21±0.87
Beit Shemesh	31.25	34.75	0.47	96	0.84±0.24	−2.30±0.50
Beer Sheva	31.38	35.01	0.76	84	1.26±0.16	−2.52±0.76

OMI tropospheric NO_2 columns (v1.02) had a pixel center within ±0.1° latitude/longitude of the station location, and were measured under mostly-clear situations (cloud radiance fraction <50%). Only OMI observations with viewing zenith angles <35° were selected, corresponding to pixel sizes smaller than 34×14 km^2. This ensures that the satellite and surface observations coincide within 27 min solar time. The OMI pixel centers were on average within 8 km of the station locations.

retrieval algorithm has been described in detail in Boersma et al. (2007), and recent updates can be found in the DOMINO Product Specification Document (http://www.temis.nl/docs/OMI_NO2_HE5_1.0.2.pdf). Slant columns are determined with DOAS in the 405–465 nm spectral window. As for SCIAMACHY, a stratospheric slant column (from assimilation in TM4) is subtracted from the slant column, and the residual is converted into a vertical tropospheric column by the tropospheric AMF. The approach to calculate the AMF is identical to SCIAMACHY, except that different cloud retrievals are used (FRESCO+ for SCIAMACHY and O_2-O_2 (Acarreta et al., 2004) for OMI). The a priori profile shapes are sampled from the same TM4 model, at 10:00 and 13:30 h for SCIAMACHY and OMI respectively (Boersma et al., 2008a).

OMI retrieval errors have an absolute component of approximately 1.0×10^{15} molecules cm^{-2} and a relative (AMF) component of 30% (Boersma et al., 2007). The spectral fitting error is smaller for SCIAMACHY than for OMI because of better SCIAMACHY signal-to-noise ratios, but OMI errors are generally much reduced by averaging over multiple days or over multiple pixels.

2.3 Surface NO_2 concentrations

We use here near-surface concentrations of NO_2 measured every 30 minutes at 8 sites in Israel for the whole year 2006. Figure 1 and Table 1 show the station locations. Measurements are with standard chemiluminescence instruments using molybdenum oxide converters. NO_2 is catalytically converted to NO on a heated (310°C) molybdenum surface and then measured as NO by chemiluminescence after reaction with ozone. The lower detectable limit is 0.4 ppb (60 s averaging time). The molybdenum converter also partly converts other oxidized nitrogen compounds such as nitric acid (HNO_3), alkyl nitrates, and peroxyacetyl nitrate (PAN) to NO (see e.g. Steinbacher et al. (2007); Dunlea et al. (2007) and references therein). This will cause NO_2 concentrations

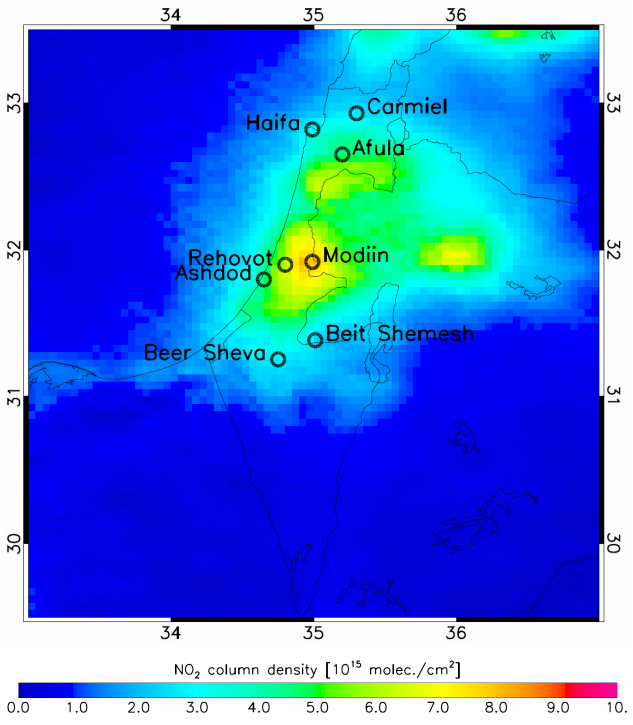

Fig. 1. Annual mean tropospheric NO_2 column in 2006 from OMI (DOMINO v1.02) for mostly-clear situations (cloud radiance fraction <50%). The circles indicate the location of surface stations.

to be overestimated, especially in photochemically aged airmasses. Steinbacher et al. (2007) have shown biases up to +50% at rural locations downwind of pollution sources in Switzerland. For urban air in Mexico City, Dunlea et al. (2007) find no significant bias in the morning but increasing bias in the afternoon, presumably reflecting the diurnal formation of NO_x oxidation products.

Table 2. Summary of the comparison between surface NO_2 concentrations and SCIAMACHY tropospheric NO_2 columns at 8 Israeli cities in 2006.

Station	r	n	slope (molecules cm^{-2}/ppb)	intercept (molecules cm^{-2})
Carmiel	0.69	38	1.34±0.11	−2.43±0.92
Haifa	0.43	28	0.45±0.21	−4.31±1.57
Afula	0.34	19	0.60±0.60	−0.88±1.09
Modiin	0.36	48	0.94±0.44	0.09±1.12
Rehovot	0.54	41	0.70±0.18	−0.32±0.96
Ashdod	0.61	43	0.67±0.14	−5.08±1.88
Beit Shemesh	0.49	21	1.29±0.54	−2.38±1.47
Beer Sheva	0.72	12	0.41±0.08	0.43±0.64

Comparison between uncorrected surface NO_2 concentrations and SCIAMACHY tropospheric NO_2 (v1.1) columns for 8 Israeli stations. We selected SCIAMACHY columns with a pixel center within ±0.25° latitude/longitude of the stations, measured under mostly-clear situations. The center location of the SCIAMACHY pixels (n=176) was on average within 20 km of the station location.

Recognizing that NO_y (with NO_y defined as the sum of all reactive nitrogen oxides; NO+NO_2+HNO_3+organic nitrates) is mostly NO_x within urban areas at mid-morning with little prior photochemical activity, and given the lack of evidence for morning-interference in the study by Dunlea et al. (2007), we do not correct the surface concentrations measured at 10:00 (SCIAMACHY overpass). This is further supported by CHIMERE simulations (Blond et al., 2007) over Europe that indicate that the bulk (>97%) of NO_y is NO_2 at 10:00 h within urban areas in all seasons. For measurements at 13:45 (OMI overpass) we show results from two approaches:

1. no correction, i.e. interpreting the NO_2 measurements as an upper limit for the true NO_2 concentrations;

2. correction based on the concurrently observed increase of O_3 from 10:00 to 13:45 as an indicator for the interference $\Delta[NO_z]$ (with NO_z defined as NO_y-NO_x), assuming $\Delta[NO_z]=0.1\cdot\Delta[O_3]$ on a molar basis based on Mexico City data (Dunlea et al., 2007), and with no correction if $\Delta[O_3]$ smaller or equal to 0.

3 Ensemble validation

Table 1 shows direct comparisons of OMI tropospheric NO_2 columns to surface NO_2 concentrations measured at 8 different stations in Israel at 13:30–14:00 h throughout 2006. OMI pixels with viewing zenith angles <35° have been selected, corresponding to close-to-nadir OMI pixels with sizes better than $34\times14\,km^2$. From a reduced-major axis (RMA) regression analysis (Clarke, 1980), we find the lowest slopes (0.30×10^{15}, 0.59×10^{15} molecules cm^{-2}/ppb, respectively) for the stations of Haifa and Ashdod that are situated immediately downwind of a large port (Haifa), and within 2 km of a large power plant and refinery complex (Ashdod). The other six stations are not influenced by such nearby NO_x point sources. For Afula, no summertime data were available, which reduces the range of observed values, but other than that we did not see a good reason to exclude data from Afula from our analysis. Excluding data from Haifa and Ashdod (but maintaining Afula), OMI and surface NO_2 are well-correlated (r=0.63, n=542). Correcting the 13:45 h surface NO_2 observations for NO_z interference as described above, leads to surface NO_2 concentrations that are on average smaller by 8%, or approximately 0.7 ppb. We evaluated our interference corrections with the CHIMERE chemistry-transport model (Blond et al., 2007) over Europe, taking advantage of its high-resolution (0.25° longitude × 0.125° latitude). In urban areas with NO_2 concentrations similar to those observed in Israeli cities (0–25 ppb), the simulated NO_2:NO_z ratio at 14:00 exceeds 0.92 for all seasons, suggesting that interference from NO_z is generally smaller than 10% in urban regions. For January, April, July, and October, NO_2:NO_z ratios were [0.98, 0.96, 0.92, 0.97], and correction factors derived from CHIMERE with the Dunlea et al. (2007)-approach described in Sect. 2.3 are similar ([0.99, 0.98, 0.95, 0.98]). For the observations in Israeli cities, application of the Dunlea et al. (2007)-approach results in correction factors of [0.91, 0.91, 0.95, 0.90]. Both direct simulations (NO_2:NO_z) and simulations with the Dunlea et al. (2007)-approach, as well as observations with the Dunlea et al. (2007)-approach within Israeli cities agree that interference from NO_z is generally smaller than 10% in urban regions. We compared correction factors simulated with CHIMERE against observed correction factors over the rural area of Taenikon (as published in Lamsal et al. (2008)), and found good agreement (CHIMERE: [0.89, 0.55, 0.44, 0.75], observations: [0.85, 0.54, 0.50, 0.80]). We conclude that a correction for interference from NO_z in the early afternoon is much more urgent in rural areas with relatively high abundance of oxidized nitrogen oxides than in urban regions, where NO_x dominates the NO_y budget.

Table 2 shows comparisons of NO_2 concentrations measured at 10:00 to SCIAMACHY tropospheric NO_2. For the

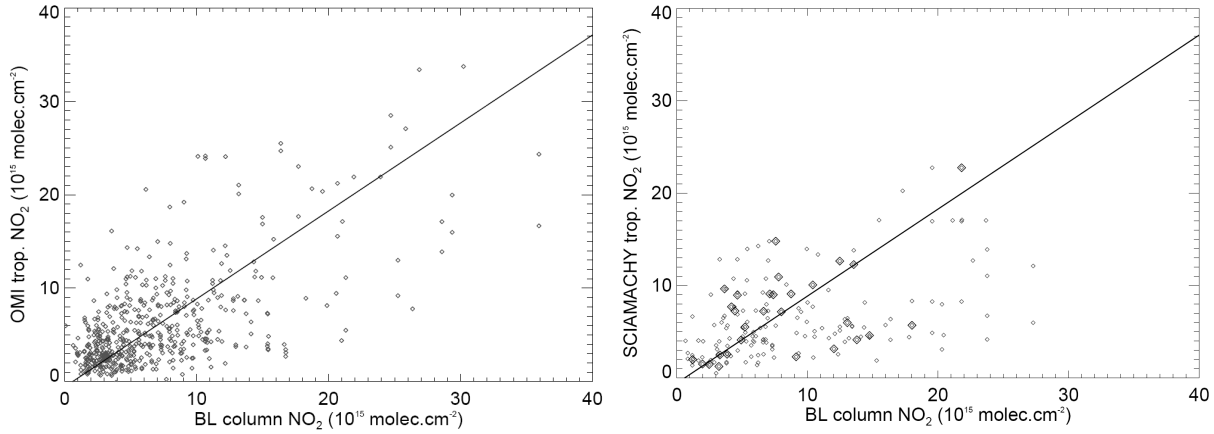

Fig. 2. Left panel: OMI tropospheric versus interference-corrected boundary layer NO_2 columns (10^{15} molecules cm^{-2}) at 13:30–14:00 h at 6 Israeli stations. The solid line indicates the result of a RMA regression (r=0.63, slope=0.93). OMI measurements have been taken under mostly clear conditions (cloud radiance fraction <50%) and with pixel centres within 0.1° of the stations. Right panel: same, but now for SCIAMACHY and boundary layer NO_2 columns at 10:00 h. The solid line indicates the RMA regression to SCIAMACHY (cloud radiance fraction <50%) observations within 0.1° of the stations, indicated by the larger diamonds (r=0.54, slope=0.94). The smaller diamonds indicate coincidences where SCIAMACHY pixel centers were within 0.25° of the stations.

locations of Haifa and Ashdod, correlations and slopes are low, consistent with their situation downwind of strong point sources and with the results found for OMI (Table 1). The agreement between SCIAMACHY and surface NO_2 amounts to r=0.48 (n=173). Sharpening the spatial coincidence criterion to ±0.1°, as for OMI, improves the correlation (r=0.55) between surface and SCIAMACHY NO_2, at the expense of the number of coincidences (n=29).

We derive BL NO_2 columns from the near-surface NO_2 mixing ratios by assuming vertical uniformity in the BL (using GEOS-Chem) and negligible concentrations above. We take the noontime mixing depths for Israel from a climatology of mixing depth observations (Table 2 in Dayan et al. (1988)) with noontime mixing depths of [1.12, 0.87, 0.65, 0.95] km for winter, spring, summer, and fall respectively. Mixing depths in Israel are minimum in summer due to strong subsidence, and have an uncertainty of ≈25% (Dayan et al., 2002). Neglecting NO_2 above the BL is a reliable assumption (Martin et al., 2002; Boersma et al., 2008b), that we evaluated further with GEOS-Chem. GEOS-Chem simulates free-tropospheric NO_2 columns over Israel that range from 0.1×10^{15} molecules cm^{-2} in winter to 0.4×10^{15} molecules cm^{-2} in summer, presumably from the stronger lightning NO_x source in that season. For the urban regions studied here, this implies on average a <8% free tropospheric contribution to the tropospheric column in Summer and <2% in Winter, small enough to be neglected. We also evaluated our assumption of vertical uniformity in the boundary layer by comparing BL columns assuming constant mixing ratios throughout the boundary layer, to the BL columns we obtained thusfar (these assumed vertical uniformity following the well-mixed GEOS-Chem boundary layer that also accounts for the decrease of NO_2/NO ratio with temperature). On average, BL NO_2 columns obtained by extrapolating surface mixing ratios throughout the BL are 13% higher than obtained by using the more realistic GEOS-Chem scheme.

Figure 2 compares tropospheric NO_2 columns retrieved from OMI and SCIAMACHY with interference-corrected BL NO_2 columns derived from near-surface measurements. As seen in the left panel, BL NO_2 columns show a similar correlation with OMI (r=0.64, n=542) as the surface concentrations (r=0.63). The slope of the RMA regression is 0.93±0.06 and the intercept is -0.37×10^{15} molecules cm^{-2}, indicating that on average OMI does not deviate significantly from the BL NO_2 columns. This is supported by sensitivity tests with alternative BL columns computed by (a) not correcting for interference (r=0.67, slope 0.90), (b) accounting for free tropospheric NO_2 from GEOS-Chem (r=0.64, slope 0.93), and (c) assuming constant mixing ratios throughout the BL (r=0.64, slope 0.81). In all three cases, the validation results are similar to our best estimate presented above. The right panel of Fig. 2 shows the agreement between SCIAMACHY and BL NO_2 (r=0.46, n=173). Selecting pixels within ±0.1°, as for OMI, improves the correlation (r=0.54, slope=0.94) between BL and SCIAMACHY NO_2 columns.

4 Temporal variability

4.1 Annual cycle

Figure 3 shows the seasonal variation of NO_2 over Israel in 2006 for the five stations with comparable NO_2 concentrations and seasonal variations and year-round coverage (all

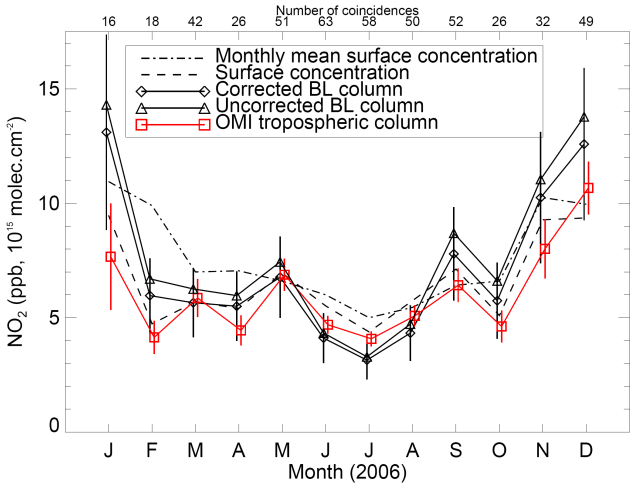

Fig. 3. Seasonal variation of NO_2 (2006) observed in Israel cities. The dashed-dotted line indicates the monthly mean near-surface NO_2 concentration for all conditions (including cloudy). The dashed line indicates the subset for mostly-clear satellite-coincidences only (cloud radiance fractions $<$50%). The solid black lines indicate the boundary layer NO_2 columns inferred from the surface concentrations with (diamonds) and without (triangles) interference correction. OMI tropospheric NO_2 columns in red. The error bars represent the standard deviation of the mean values. The numbers in the upper x-axis refer to the number of cloud-free coincidences found in each month.

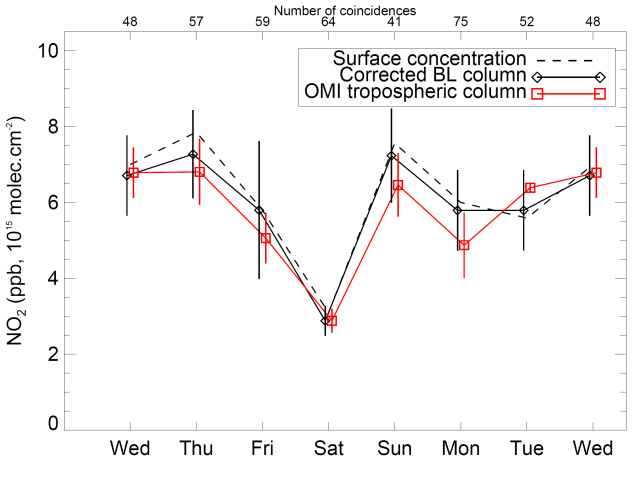

Fig. 4. Weekly variation of NO_2 over Israeli cities, March-November 2006. The dashed line indicates the mean NO_2 observed near-surface, the black diamonds represent interference-corrected surface measurements, and OMI observations are in red squares. All curves for the Israeli stations of Beer Sheva, Beit Shemesh, Carmiel, Rehovot, and Modiin. Winter measurements have been excluded to avoid sampling biases (some weekdays had no winter measurements). The numbers in the upper x-axis refer to the number of cloud-free coincidences found for each day.

except Ashdod, Haifa, and Afula; for the latter no summer-data were available). The dashed-dotted line is for all surface measurements including cloudy conditions. The black dashed line is for measurements coinciding with satellite data, i.e. measured under mostly-clear conditions only. Exclusion of cloudy scenes in the validation data subset decreases concentrations by 15% on average but does not affect the seasonal variation.

Both OMI (red squares) and boundary-layer NO_2 columns (black symbols) are highest in the winter months, presumably reflecting the seasonal variation of NO_2 lifetime. We see that monthly mean NO_2 columns from the in situ observations and from OMI are similar within their error margins for all months. For the boundary-layer columns, error bars mainly reflect the uncertainty in the boundary-layer depths (25%, based on estimates from Dayan et al. (1988)). If there is a bias in the BL-depths, it directly propagates into our BL column estimates, and this could explain the large differences between BL columns and OMI in winter. For OMI, error bars indicate the standard deviation of the mean. The seasonal cycle, expressed as the ratio of winter-to-summer mean NO_2, is 2.7 ± 0.6 in the boundary-layer NO_2 columns, and 1.6 ± 0.5 in surface and OMI NO_2.

4.2 Weekly cycle

The weekly cycle of coinciding ground-based and OMI NO_2 is shown in Fig. 4 for five stations in the period between March and November 2006 (Afula was rejected because no summertime data were available). Wintertime observations have been excluded because in this season no coincidences were available for Saturdays. The weekly cycle is due to reduced NO_x emissions on Fridays and Saturdays corresponding to the weekend pattern and days of rest. We observe reductions in NO_2 on Friday and Saturday in surface NO_2 concentrations (dashed line), corrected BL NO_2 columns (black diamonds), as well as in OMI NO_2 columns (red squares). The reduction on Saturday is significant, 50% relative to the weekday mean. Beirle et al. (2003) observed a similar Saturday NO_2 reduction over Israel on the regional scale from GOME. Their reduction (30%) is smaller because the relatively large GOME pixel ($320\times40\,km^2$) covers not just the strong source region of Israel, but also adjacent parts of the Mediterranean Sea and Jordan where sources are weaker and less likely to show a distinct weekend effect. In contrast, the small-pixel OMI observations used here are representative for the urban scale and more likely to show the local weekend emission reductions.

Table 3. The 10:00–13:45 ratios of tropospheric NO_2 columns for source regions in the Middle East.

Region	Corner coordinates	winter	spring	summer	autumn
Israel	31.0–33.0° N, 34.5–35.5° E	0.77	1.00	1.29	0.88
Cairo	29.0–30.5° N, 30.5–32.0° E	0.91	1.16	1.16	1.12

Ratios calculated as geometrical means shown in Fig. 6a–d.

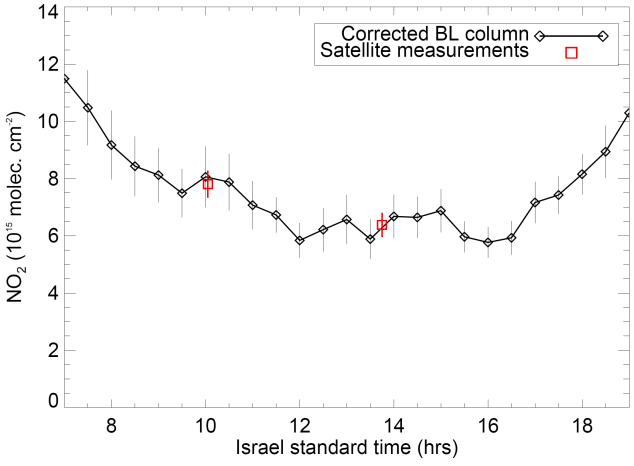

Fig. 5. Diurnal variation of NO_2 in Israeli cities in March-November 2006. The black diamonds indicate the mean (n=35) boundary layer NO_2 columns observed with 30-min intervals, with coincident and collocated SCIAMACHY and OMI NO_2 columns in red. All columns have been observed on the same cloud-free days at the locations of Israeli surface stations. The pixel centre latitudes and longitudes were required to be within 0.1° (OMI), 0.25° (SCIAMACHY) of the station locations.

4.3 Diurnal cycle

Figure 5 shows average NO_2 columns measured at the locations of the Israeli stations (except Ashdod, Haifa, and Afula) on the same days at 10:00 and 13:45 in cloud-free conditions in the period March–November 2006. BL and satellite-retrieved NO_2 columns are consistent at 10:00 and at 13:45. The geometric mean of the ratio of SCIAMACHY and OMI NO_2 columns over Israeli cities is 1.22, and this tendency is quantitatively consistent with the geometric mean of 1.18 of 10:00 and 13:45 surface-based NO_2 columns. It is unlikely that these results are due to retrieval differences, as SCIAMACHY and OMI NO_2 columns have been retrieved with a consistent algorithm (Boersma et al., 2008a), and both datasets agree well with the independent data shown in Fig. 5. The results appear consistent with findings of Boersma et al. (2008a) over fossil fuel source regions at northern mid-latitudes, where SCIAMACHY observed 5–40% higher NO_2 than OMI in summer, explained by daytime photochemical loss of NO_2, dampened by the diurnal cycle of anthropogenic NO_x emissions that has a broad daytime maximum. Comparing 10:00 and 13:45 NO_2 observed on the same days during winter months in Israel did not show the same diurnal cycle, and we will now investigate this further.

Figure 6a–d shows seasonally averaged differences between SCIAMACHY and OMI tropospheric NO_2 measured on the same day in mostly clear conditions over Israel and the surrounding regions in 2006 on a $0.5° \times 0.5°$ grid. The inset shows the corresponding scatter plot with the Israeli grid cells marked in light blue. For comparison to a nearby industrialized region, we also plotted the Cairo grid cells, in red. In winter (DJF, 2006), when NO_2 lifetimes are longest and NO_2 columns largest, we see in Fig. 6a that SCIAMACHY tends to observe similar or lower NO_2 amounts at 10:00 than OMI at 13:45 h over the NO_x source regions of Israel and Cairo. The geometrical mean ratios are <1.0 for both Israel and Cairo as indicated by the solid light blue and red lines in the inset. In summer, with shorter chemical lifetimes and smaller NO_2 columns than in winter, we see the reverse effect in Fig. 6c with 10:00–13:45 ratios of 1.29 over Israel and 1.16 over Cairo. Spring and autumn show diurnal variations in between the winter and summer extremes. Table 3 summarizes the mean 10:00–13:45 ratios for all seasons.

To evaluate this apparent seasonal cycle in the diurnal cycle, we compare ratios of NO_2 at 10:00 and 13:45 observed from satellites and from surface stations. We do not require spatial or temporal coincidence between satellite and surface measurements (as we did before), but only that both techniques measured under mostly-clear situations. The top panel of Fig. 7 shows significant 10:00–13:45 decreases in both satellite and surface-based observations over Israel in summer, and no decrease, or even a slight increase, in winter months. This is consistent with simulations from the 3-D chemistry-transport model GEOS-Chem (Bey et al., 2001) for the same location and time, as shown in the bottom panel of Fig. 7. In summer, GEOS-Chem simulates up to 21% higher NO_2 columns at 10:00, compared to smaller differences in winter. That the GEOS-Chem summertime ratios are smaller than observed by the two measurement techniques, is explained by the spatial extent of the GEOS-Chem grid cell ($2° \times 2.5°$). The GEOS-Chem grid cell covers not only the region of Israel where NO_x sources are strong, but also a large part of the Mediterranean Sea where these sources are weak. To bridge the gap between the simulation and the higher-resolution observations, we sampled the

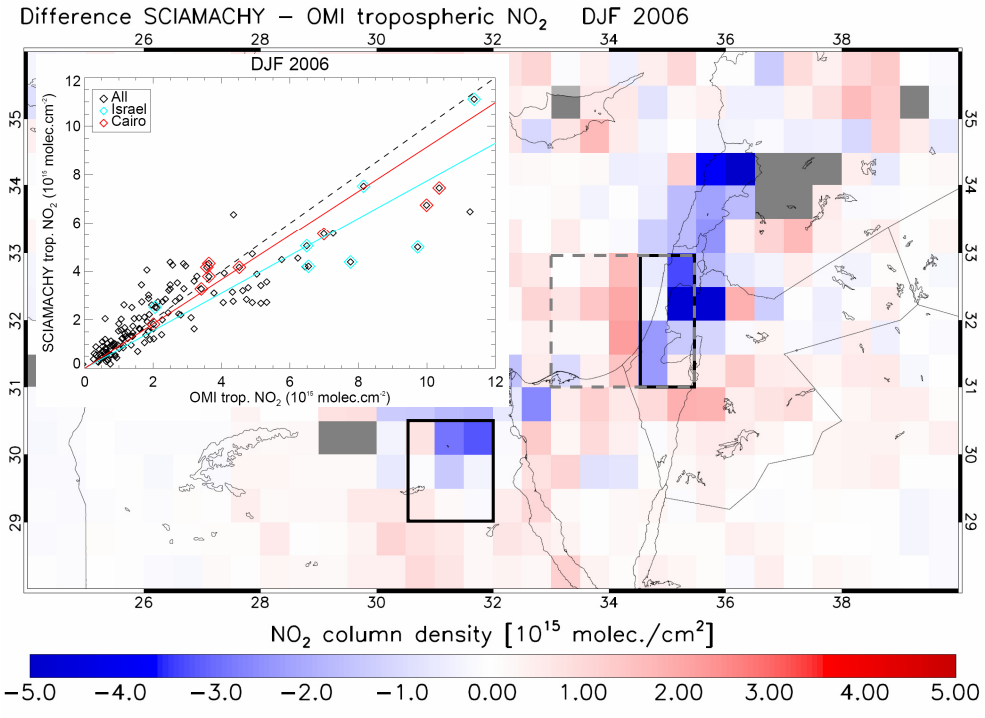

Fig. 6a. Absolute difference between SCIAMACHY and OMI tropospheric NO_2 columns over the Middle East in winter 2006. Red colors indicate higher retrievals from SCIAMACHY than from OMI, and vice versa for blue colors. The measurements have been taken under mostly clear conditions. The inset shows the corresponding scatter plot. The light blue diamonds indicate the grid cells over Israel, and the red ones over the greater Cairo region. The dashed line in the inset represents $y=x$. The solid light blue and red lines illustrate the corresponding geometrical mean SCIAMACHY:OMI ratio over Israel and Cairo. Both regions are enclosed by the black rectangles in the map. The region enclosed by the grey dashed rectangle represents the spatial extent of the GEOS-Chem grid cell over Israel.

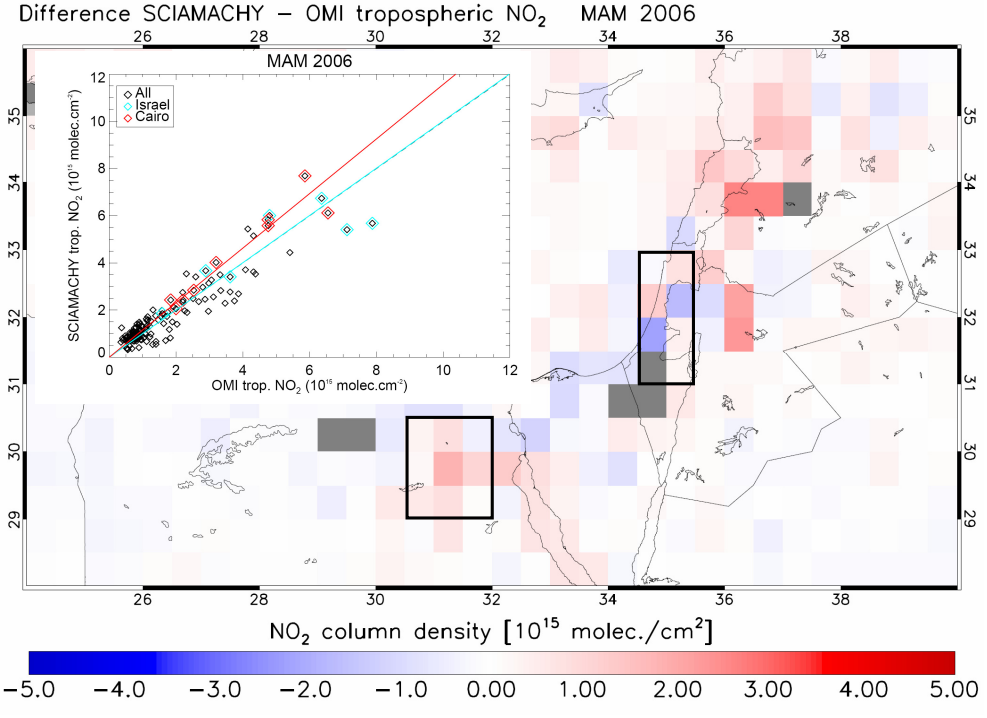

Fig. 6b. Same as Fig. 6a, but now for spring (March, April, May) 2006.

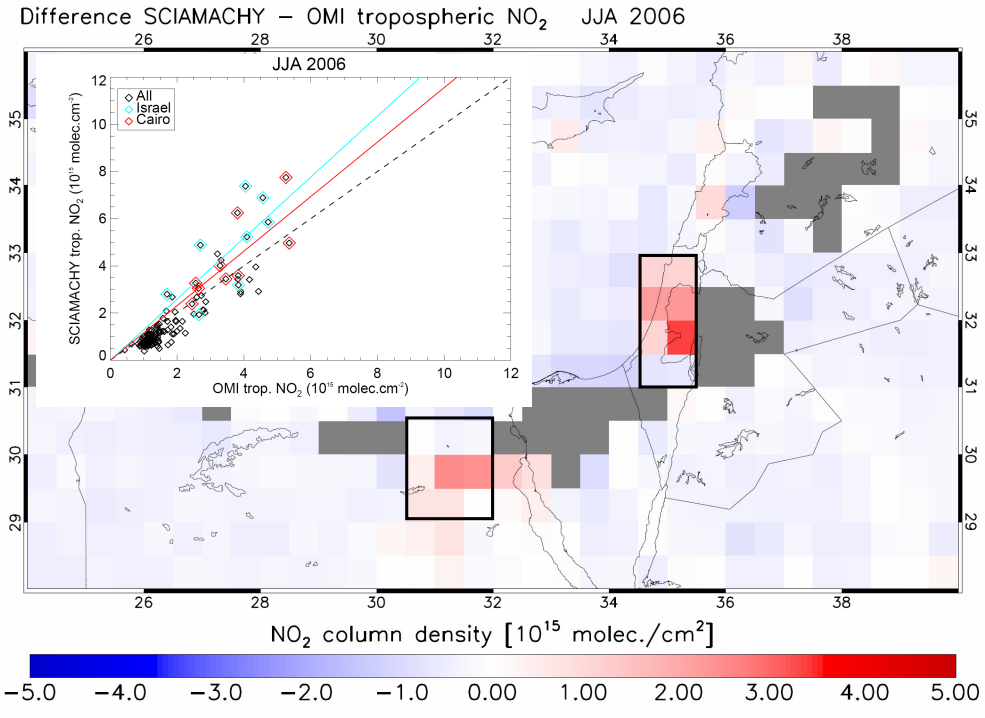

Fig. 6c. Same as Fig. 6a, but now for summer (June, July, August) 2006.

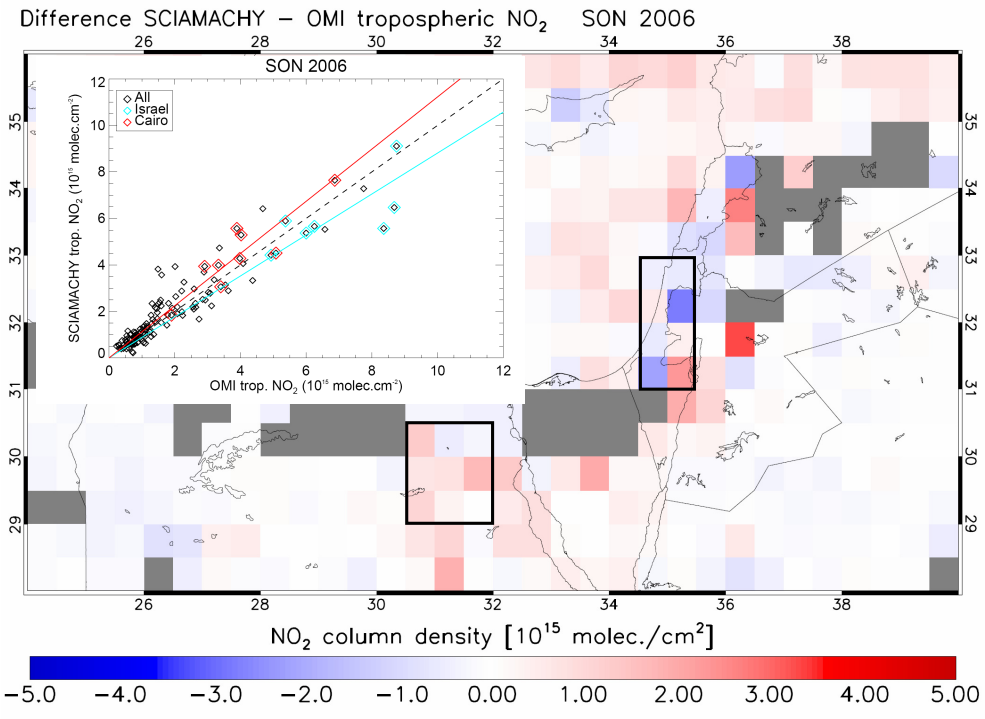

Fig. 6d. Same as Fig. 6a, but now for autumn (September, October, November) 2006.

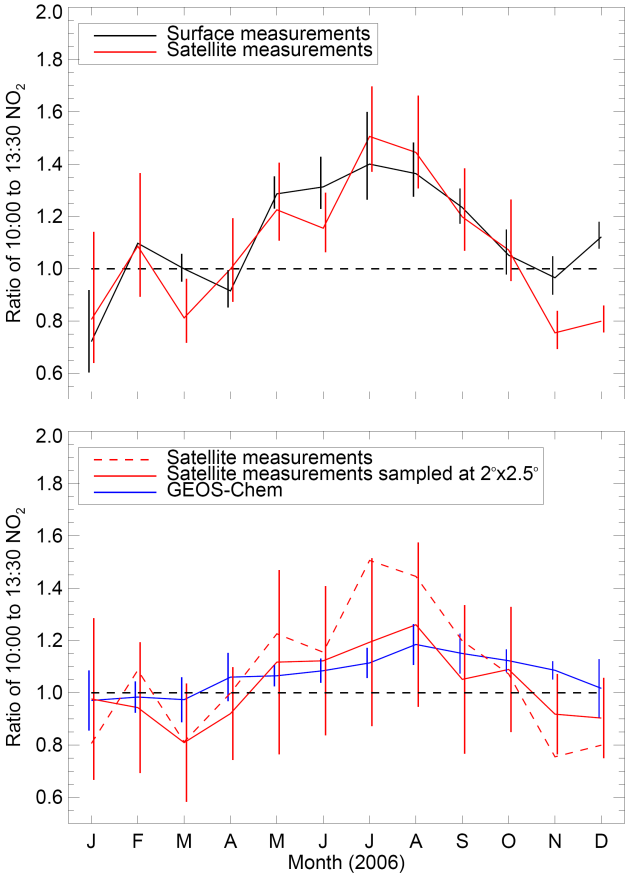

Fig. 7. Seasonal cycle in the diurnal cycle of tropospheric NO_2 columns. Upper panel: cycle over the Israel source region from surface measurements (black line), and from SCIAMACHY and OMI measurements (red line). Lower panel: cycle over the $2° \times 2.5°$ area of the GEOS-Chem grid cell from satellite measurements (solid red line) and from the GEOS-Chem model sampled at 10:00 and 13:30 h (solid blue line).

satellite measurements according to the boundaries of the GEOS-Chem grid cell. The seasonal cycle in the diurnal cycle observed at $2° \times 2.5°$ (solid red curve) agrees much better with the GEOS-Chem simulations than the high-resolution curve ($2° \times 1°$, dashed line).

The diurnal variation of tropospheric NO_2 columns depends on the diurnal cycle of NO_x emissions and chemical loss (see Eq. (3) in Boersma et al. (2008a)). Over urban areas, NO_x emissions show a daytime maximum that mainly reflects intense vehicle use between early morning and late afternoon. This pattern is very similar for all seasons. In absence of strong seasonal changes in background NO_x, the seasonal variation in the diurnal cycle of tropospheric NO_2 columns can therefore be understood mainly in terms of seasonally varying photochemistry.

Figure 8 shows a GEOS-Chem simulation over Israel of the diurnal variation in the NO_2 column and in the chemical loss rate constant k for a winter and a summer month in cloud-free conditions. k includes the chemical loss of NO_x to HNO_3 through the gas-phase reaction of NO_2 with OH and the hydrolysis of N_2O_5 in aerosols. The GEOS-Chem model incorporating diurnally varying NO_x emissions and photochemistry simulates up to $5\times$ higher values and a much more pronounced diurnal cycle for k in August than in February 2006. In winter, the absence of a daytime maximum in NO_x loss is expected to lead to an increase of NO_x over the course of the day, because emissions are higher in the day than at night. The seasonal differences in k are consistent with higher OH concentrations in summer reflecting higher water vapour concentrations and more UV flux in that season (Spivakovsky et al., 2000). It is this strong daytime change in k (OH) in summer that is responsible for the distinct decrease in the NO_2 columns between 10:00 and 13:45 in summer. In winter, the chemical loss rate constant is generally too small throughout the day (low OH) to yield a net chemical loss, implying that NO_x emissions may offset chemical loss during the daylight hours in that season. It is this mechanism that likely explains the observed wintertime 10:00–13:45 increases (expressed as ratios <1.0) in Fig. 7.

5 Conclusions

We showed that NO_2 concentration data from urban monitoring networks can provide useful validation for NO_2 column measurements from space. Previous validations of satellite retrievals relied primarily on profile measurements from aircraft, but these do not sample the lowest part of the atmosphere, where most of the NO_2 resides and strong gradients exist, and provide little statistics needed to overcome difficulties in vertical extrapolation and horizontal representativity. Ground-based measurements on the other hand sample NO_2 close to the source and offer the benefit of large, continuous datasets.

Our validation focused on urban locations in Israel in 2006. In situ measurements (10:00 and 13:45 h) of NO_2 concentrations show significant correlation with collocated SCIAMACHY and close-to-nadir OMI tropospheric NO_2 column retrievals. We converted surface concentrations into columns representative for the boundary layer (BL) by assuming a well-mixed BL, and a climatology of observed Israeli BL depths. Afternoon surface NO_2 has been corrected for potential interference from oxidized nitrogen compounds (NO_z). This correction leads to 5–15% smaller NO_2 concentrations. The collocated 13:45 hrs BL and OMI NO_2 columns are in agreement (r=0.64, n=542, slope=0.93±0.06). A similar agreement is apparent in 10:00 h BL and SCIAMACHY NO_2 columns, provided they were collocated within 0.1°.

The observed seasonal cycles in ground-based measurements and OMI NO_2 are consistent. BL and OMI NO_2 columns are $1.6–2.7\times$ higher in winter than in summer, reflecting the strong seasonal variation in photochemistry and NO_2 lifetime. OMI observes a strong weekly cycle with

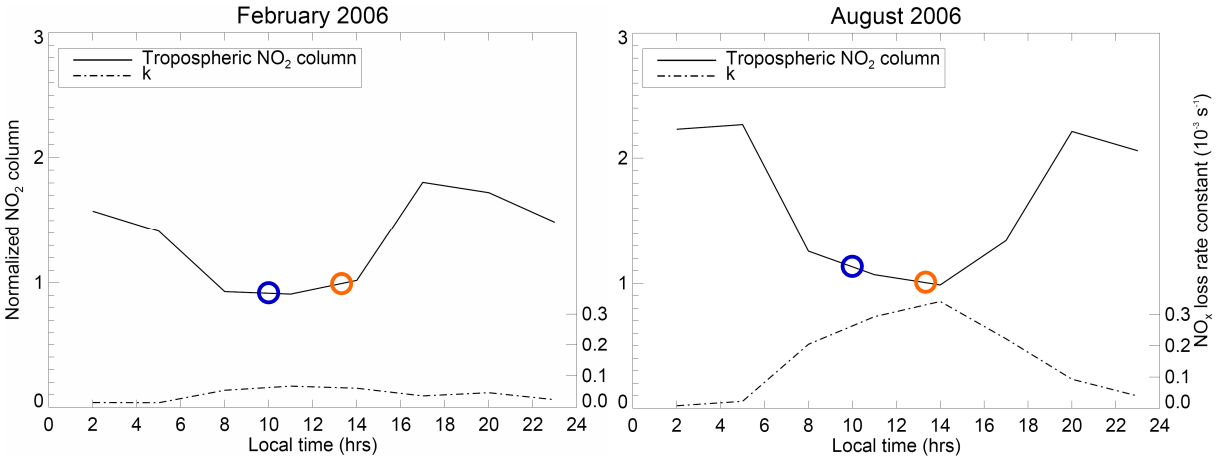

Fig. 8. Diurnal cycle in tropospheric NO_2 columns (solid line) and NO_x chemical loss rate constant k (dashed line) over Israel, simulated by GEOS-Chem for mostly-clear conditions in February 2006 (left panel), and August 2006 (right panel). The open circles indicate the value of the simulated tropospheric NO_2 column at the SCIAMACHY (blue) and OMI (orange) overpass times.

approximately 50% smaller NO_2 columns on the Saturdays relative to the weekday mean. Ground-based techniques observe 46% lower NO_2 on Saturdays, similar as from space.

Outside the winter season, collocated satellite and ground-based measurements show higher NO_2 columns at 10:00 than at 13:45. In summer, the diurnal variation is strongest, with 10:00–13:45 ratios up to 1.4. In winter, the observed ratios are close to 1.0, and there is often a (small) increase in tropospheric NO_2 between mid-morning and early afternoon. Simulations with the global 3-D chemical transport model GEOS-Chem are consistent with the observed seasonal variation in the 10:00 vs. 13:45 difference. The simulations suggest that the high summertime and low wintertime ratios can be understood from a much stronger photochemical sink from oxidation by OH in summer than in winter. In winter, the photochemical sink is sufficiently small that continuous NO_x emissions may offset chemical loss during the daylight hours, explaining the observed 10:00–13:45 increase in NO_2.

The quality of the satellite retrievals at the urban scales shown here provides some confidence in top-down constraints on NO_x emissions from the satellite data. But retrievals should be improved by using forward model parameters (surface albedo's, a priori profile shapes, and surface pressures) from data bases with horizontal resolutions similar to the satellite footprints. Aerosols contribute to retrieval uncertainty because they affect retrieved cloud fractions, and this complex interaction should be investigated further in order to reduce retrieval errors.

Acknowledgements. This work was funded by the NASA Atmospheric Composition Modeling and Analysis Program. The OMI project is managed by NIVR and KNMI in The Netherlands. The ground level data was provided by the Israel Ministry of Environmental Protection. Yinon Rudich acknowledges support by the Helen and Martin Kimmel Award for Innovative Investigation. This research was partially supported by Research Grant Award No. RGA0803 from the Environmental and Health Fund, Jerusalem, Israel. We thank two anonymous reviewers, whose comments helped improve this work.

Edited by: B. Duncan

References

Acarreta, J. R., de Haan, J. F., and Stammes, P.: Cloud pressure retrieval using the O_2-O_2 absorption band at 477 nm, J. Geophys. Res., 109, D05204, doi:10.1029/2003JD003915, 2004.

Beirle, S., Platt, U., Wenig, M., and Wagner, T.: Weekly cycle of NO_2 by GOME measurements: a signature of anthropogenic sources, Atmos. Chem. Phys., 3, 2225–2232, 2003, http://www.atmos-chem-phys.net/3/2225/2003/.

Bey, I., Jacob, D. J., Yantosca, R. M., Logan, J. A., Field, B. D., Fiore, A. M., Li, Q., Liu, H. Y., Mickley, L. J., and Schultz, M. G.: Global modeling of tropospheric chemistry with assimilated meteorology: Model description and evaluation, J. Geophys. Res., 106, 23073–23096, 2001.

Blond, N., Boersma, K. F., Eskes, H. J., van der A, R. J., Van Roozendael, M., De Smedt, I., Bergamatti, G., and Vautard, R.: Intercomparison of SCIAMACHY nitrogen dioxide observations, in situ measurements and air quality modeling results over Western Europe, J. Geophys. Res., 112, D10311, doi:10.1029/2006JD007277, 2007

Boersma, K. F., Eskes, H. J., and Brinksma, E. J.: Error analysis for tropospheric NO_2 retrieval from space, J. Geophys. Res., 109, D04311, doi:10.1029/2003JD003962, 2004.

Boersma, K. F., Eskes, H. J., Veefkind, J. P., Brinksma, E. J., van der A, R. J., Sneep, M., van den Oord, G. H. J., Levelt, P. F., Stammes, P., Gleason, J. F., and Bucsela, E. J.: Near-real time retrieval of tropospheric NO_2 from OMI, Atmos. Chem. Phys., 7, 2103–2118, 2007, http://www.atmos-chem-phys.net/7/2103/2007/.

Boersma, K. F., Jacob, D. J., Eskes, H. J., Pinder, R. W., Wang, J., and van der A, R. J.: Intercomparison of SCIAMACHY and

OMI tropospheric NO_2 columns: Observing the diurnal evolution of chemistry and emissions from space, J. Geophys. Res., 113, D16S26, doi:10.1029/2007JD008816, 2008a.

Boersma, K. F., Jacob, D. J., Bucsela, E. J., Perring, A. E., Dirksen, R., van der A, R. J., Yantosca, R. M., Park, R. J., Wenig, M. O., Bertram, T. H., and Cohen, R. C.: Validation of OMI tropospheric NO_2 observations during INTEX-B and application to constrain NO_x emissions over the eastern United States and Mexico, Atmos. Environm., 42(19), 4480–4497, doi:10.1026/j.atmosenv.2008.02.004, 2008b.

Bucsela, E. J., Perring, A. E., Cohen, R. C., Boersma, K. F., Celarier, E. A. Gleason, J. F., Wenig, M. O., Bertram, T. H., Wooldridge, P. J., Dirksen, R., and Veefkind, J. P.: Comparison of tropospheric NO_2 from in-situ aircraft measurements with near-real time and standard product data from OMI, J. Geophys. Res., 113, D16S31, doi:10.1029/2007JD008838, 2008.

Clarke, M. R. B.: The reduced major axis of a bivariate sample, Biometrika, 67(2), 441–446, 1980.

Dayan, U., Shenhav, R., and Graber, M.: The Spatial and Temporal Behavior of the Mixed Layer in Israel, J. Appl. Meteor., 27, 1382–1394, 1988.

Dayan, U., Lifshitz-Goldreich, B., and Pick, K.: Spatial and Structural Variation of the Atmospheric Boundary Layer during Summer in IsraelProfiler and Rawinsonde measurements, J. Appl. Meteor., 41, 447–457, 2002.

Dentener, F., Peters, W., Krol, M. van Weele, M., Bergamaschi, P., and Lelieveld, J., Interannual variability and trend of CH_4 lifetime as a measure of OH changes in the 1979–2003 period, J. Geophys. Res., 108(D15), 4442, doi:10.1029/2002JD002916, 2003.

Dunlea, E. J., Herndon, S. C., Nelson, D. D., Volkamer, R. M., San Martini, F., Sheehy, P. M., Zahniser, M. S., Shorter, J. H., Wormhoudt, J. C., Lamb, B. K., Allwine, E. J., Gaffney, J. S., Marley, N. A., Grutter, M., Marquez, C., Blanco, S., Cardenas, B., Retama, A., Ramos Villegas, C. R., Kolb, C. E., Molina, L. T., and Molina, M. J.: Evaluation of nitrogen dioxide chemiluminescence monitors in a polluted urban environment, Atmos. Chem. Phys., 7, 2691–2704, 2007, http://www.atmos-chem-phys.net/7/2691/2007/.

Ellis, E. C.: Technical assistance document for the chemiluminescence measurement of nitrogen dioxide, Environmental Monitoring and Support Laboratory, U.S. Environmental Protection Agency, EPA-600/4-75-003, 1975.

Gerboles, M., Lagler, F., Rembges, D., and Brun, C.: Assessment of uncertainty of NO_2 measurements by the chemiluminescence method and discussion of the quality objective of the NO_2 European Directive, J. Environ. Monit., 5, 529–540, 2003.

Grosjean, D. and Harrison, J.: Response of chemiluminescence NO_x analyzers and ultraviolet ozone analyzers to organic air pollutants, Environ. Sci. Technol., 19, 862–865, 1985.

Heland, J., Schlager, H., Richter, A., and Burrows, J. P.: First comparison of tropospheric NO_2 column densities retrieved from GOME measurements and in situ aircraft profile measurements, Geophys. Res. Lett., 29(20), 1983, doi:10.1029/2002GL015528, 2002.

Hjellbrekke, A.-G. and Fjæraa, A. M.: Acidifying and eutrophying compounds and particulate matter, Data Report 2006, EMEP/CCC-Report 1/2008, Kjeller, Norwegian Institue for Air Research, 2008.

IPCC, 2007: Climate Change 2007: The Physical Science Basis. Contribution of Working Group I to the Fourth Assessment Report of the Intergovernmental Panel on Climate Change, edited by: Solomon, S., Qin, D., Manning, M., Chen, Z., Marquis, M., Averyt, K. B., Tignor, M., and Miller, H. L., Cambridge University Press, Cambridge, United Kingdom and New York, NY, USA, 996 pp., 2007.

Konovalov, I. B., Beekmann, M., Richter, A., and Burrows, J. P.: Inverse modelling of the spatial distribution of NOx emissions on a continental scale using satellite data, Atmos. Chem. Phys., 6, 1747–1770, 2006, http://www.atmos-chem-phys.net/6/1747/2006/.

Krijger, J. M., van Weele, M., Aben, I., and Frey, R.: Technical Note: The effect of sensor resolution on the number of cloud-free observations from space, Atmos. Chem. Phys., 7, 2881–2891, 2007, http://www.atmos-chem-phys.net/7/2881/2007/.

Lamsal, L. N., Martin, R. V., van Donkelaar, A., Steinbacher, M., Celarier, E. A., Bucsela, E., Dunlea, E. J., and Pinto, J. P.: Ground-level nitrogen dioxide concentrations inferred from the satellite-borne Ozone Monitoring Instrument, J. Geophys. Res., 113, D16308, doi:10.1029/2007JD009235, 2008.

Liang, J., Horowitz, L. W., Jacob, D. J., Wang, Y., Fiore, A. M., Logan, J. A., Gardner, G. M., and Munger, J. W.: Seasonal budgets of reactive nitrogen species and ozone over the United States, and export fluxes to the global atmosphere, J. Geophys. Res., 103(D11), 13435–13450, 1998.

Martin, R. V., Chance, K., Jacob, D. J., Kurosu, T. P., Spurr, R. J. D., Bucsela, E., Gleason, J. F., Palmer, P. I., Bey, I., Fiore, A. M., Li, Q., Yantosca, R. M., and Koelemeijer, R. B. A.: An improved retrieval of tropospheric nitrogen dioxide from GOME, J. Geophys. Res., 107(D20), 4437, doi:10.1029/2001JD001027, 2002.

Martin, R. V., Jacob, D. J., Chance, K. V., Kurosu, T. P., Palmer, P. I., and Evans, M. J.: Global inventory of Nitrogen Dioxide Emissions Constrained by Space-based Observations of NO_2 Columns, J. Geophys. Res., 108, 4537, doi:10.1029/2003/JD003453, 2003.

Martin, R. V., Parrish, D. D., Ryerson, T. B., Nicks Jr., D. K., Chance, K., Kurosu, T. P., Jacob, D. J., Sturges, E. D., Fried, A., and Wert, B. P.: Evaluation of GOME satellite measurements of tropospheric NO_2 and HCHO using regional data from aircraft campaigns in the southeastern United States, J. Geophys. Res., 109, D24307, doi:10.1029/2004JD004869, 2004.

Martin, R. V., Sioris, C. E., Chance, K., Ryerson, T. B., Bertram, T. H., Wooldridge, P. J., Cohen, R. C., Neuman, J. A., Swanson, A., and Flocke, F. M.: Evaluation of space-based constraints on global nitrogen oxide emissions with regional aircraft measurements over and downwind of eastern North America, J. Geophys. Res., 111, D15308, doi:10.1029/2005JD006680, 2006.

Ordóñez, C., Richter, A., Steinbacher, M., Zellweger, C., N¨ss, H., Burrows, J. P., and Prévôt, A. S. H.: Comparison of 7 years of satellite-borne and ground-based tropospheric NO_2 measurements around Milan, Italy, J. Geophys. Res., 111, D05310, doi:10.1029/2005JD006305, 2006.

Richter, A., Eyring, V., Burrows, J. P., Bovensmann, H., Lauer, A., Sierk, B., and Crutzen, P. J.: Satellite measurements of NO_2 from international shipping emissions, Geophys. Res. Lett., 31, L23110, doi:10.1029/2004GL020822, 2004.

Schaub, D., Boersma, K. F., Kaiser, J. W., Weiss, A. K., Folini, D., Eskes, H. J., and Buchmann, B.: Comparison of GOME tropospheric NO_2 columns with NO_2 profiles deduced from ground-based in situ measurements, Atmos. Chem. Phys., 6, 3211–3229, 2006,
http://www.atmos-chem-phys.net/6/3211/2006/.

Steinbacher, M., Zellweger, C., Schwarzenbach, B., Bugmann, S., Buchmann, B., Ordóñez, C., Prévôt, A. S. H., and Hueglin, C.: Nitrogen oxide measurements at rural sites in Switzerland: Bias of convential measurement techniques, J. Geophys. Res., 112, D11307, doi:10.1029/2006JD007971.

Spivakovsky, C. M., Logan, J. A., Montzka, S. A., Balkanski, Y. J., Foreman-Bowler, M., Jones, D. B. A., Horowitz, L. W., Fusco, A. C., Brenninkmeijer, C. A. M., Prather, M. J., Wofsy, S. C., and McElroy, M. B.: Three-dimensional climatological distribution of tropospheric OH: Update and evaluation, J. Geophys. Res., 105(D7), 8931–8980, 2000.

van der A, R. J., Eskes, H. J., Boersma, K. F., van Noije, T. P. C., Van Roozendael, M., De Smedt, I., Peters,D. H. M. U., and Meijer, E. W.: Trends, seasonal variability and dominant NO_x source derived from a ten year record of NO_2 measured from space, J. Geophys. Res., 113, D04302, doi:10.1029/2007JD009021, 2008.

Wang, Y. X., McElroy, M. B., Boersma, K. F., Eskes, H. J., and Veefkind, J. P.: Traffic Restrictions Associated with the Sino-African Summit: Reductions of NO_x Detected from Space, Geophys. Res. Lett., 34, L08814, doi:10.1029/2007GL029326, 2007.

Wang, P., Stammes, P., van der A, R., Pinardi, G., and van Roozendael, M.: FRESCO+: an improved O_2 A-band cloud retrieval algorithm for tropospheric trace gas retrievals, Atmos. Chem. Phys., 8, 6565–6576, 2008,
http://www.atmos-chem-phys.net/8/6565/2008/.

Winer, A. M., Peters, J. W., Smith, J. P., and Pitts, J. N.: Response of commercial chemiluminescent NO-NO_2 analyzers to other nitrogen containing compounds, Environ. Sci. Technol., 8, 1118–1121, 1974.